PACS numbers: 42.62.Eh; 42.55.Rz; 42.65.Ky
DOI: 10.1070/QE2004v034n12ABEH002851

Optical frequency standard based on a Nd : YAG laser stabilised by saturated absorption resonances in molecular iodine using second-harmonic radiation

M.N. Skvortsov, M.V. Okhapkin, A.Yu. Nevsky, S.N. Bagayev

***Abstract*. The results of studies devoted to the development of the optical frequency standard based on a diode-pumped 1064-nm single-frequency ring Nd : YAG laser with intracavity frequency doubling are presented. The laser frequency was stabilised by saturated absorption resonances in molecular iodine at the second-harmonic frequency of the laser (at 532 nm). The saturated absorption resonances were observed in an external luminescent cell. The relative long-term frequency stability achieved in experiments was $\sim 6 \times 10^{-15}$. The physical and technical factors affecting the long-term frequency stability and reproducibility are investigated.**

Keywords: *optical frequency standards, saturated absorption resonances, Nd : YAG laser, frequency stabilisation.*

1. Introduction

The 1064-nm Nd : YAG lasers are widely used in laser spectroscopy and metrology. Nd : YAG lasers stabilised by saturated absorption resonances in molecular iodine serve as radiation sources with the relative frequency stability better than 10^{-14} and are employed in ultrahigh-resolution laser spectrometers [1, 2]. There exist a variety of methods for recording saturated absorption resonances. Basov and Letokhov [3] proposed to use luminescence intensity resonances observed upon saturation absorption in a standing wave. This method offers a number of advantages in certain cases, which provide the high long-term stability and reproducibility of the laser frequency. The method of a luminescence cell was used to stabilise the Ar^+ laser frequency by saturated absorption resonances in molecular iodine at 514.5 nm [4]. In [4], the relative long-term frequency stability equal to $\Delta\nu/\nu = 5 \times 10^{-15}$ was achieved for the time $t = 100$ s and the frequency reproducibility was $\nu/\Delta\nu = 10^{13}$.

The aim of this paper is to study the possibility of the development of an optical frequency standard based on a diode-pumped 1064-nm single-frequency ring Nd : YAG laser with intracavity frequency doubling by using an external absorbing luminescence cell with molecular iodine.

M.N. Skvortsov, M.V. Okhapkin, A.Yu. Nevsky, S.N. Bagayev Institute of Laser Physics, Siberian Branch, Russian Academy of Sciences, prosp. Akad. Lavrent'eva 13/3, 630090 Novosibirsk, Russia; web-site: www.laser.nsc.ru; e-mail: skv@laser.nsc.ru

Received 9 August 2004
Kvantovaya Elektronika **34** (12) 1101 – 1106 (2004)
Translated by M.N. Sapozhnikov

2. Diode-pumped 1064-nm single-frequency ring Nd : YAG laser with intracavity frequency doubling

At present the simplest way for achieving single-frequency operation of high-power solid-state lasers is the use of travelling-wave ring resonators [5].

To obtain single-frequency operation in a longitudinally diode-pumped Nd : YAG laser, we used a unidirectional travelling wave resonator. This scheme completely eliminates the effect of spatial inhomogeneous gain saturation, which causes multimode lasing. By using a KTP crystal for intracavity frequency doubling and a temperature-tunable birefringent filter, the authors of [6] manufactured a simple laser containing a minimal number of intracavity elements, which is convenient for applications as a radiation source in the visible and IR regions.

2.1 Unidirectional lasing

A travelling wave can be generated by numerous methods. One of the most promising of them, which uses a minimal number of optical elements and, hence, features minimal intracavity losses, is the employment of an optical diode based on the Faraday effect in an amplifying medium, a partial polariser consisting, for example, of the surfaces oriented at the Brewster angle, and a nonplanar geometry (half-wave plate) as a compensator of the optical rotation of one of the counterpropagating waves [7]. In this case, optical rotation caused by a magnetic field applied to a Nd : YAG crystal is compensated by optical rotation after reflection of light from mirrors located in different planes or on the half-wave plate. In this propagation direction, losses at partial polarisers are minimal. For the counterpropagating wave, optical rotation caused by the Faraday effect in the amplifying medium is added with optical rotation at the mirrors or the half-wave plate, resulting in the enhancement of losses.

Our travelling wave Nd : YAG laser with intracavity frequency doubling and temperature tuning uses a nonplanar two-mirror resonator with a gain medium constructed in the form of a prism (Fig. 1) [6]. Output mirror (*1*) (for fundamental and second-harmonic radiations) is displaced from the BCDA′ plane. One of the surfaces of the amplifying medium is oriented at the Brewster angle and is

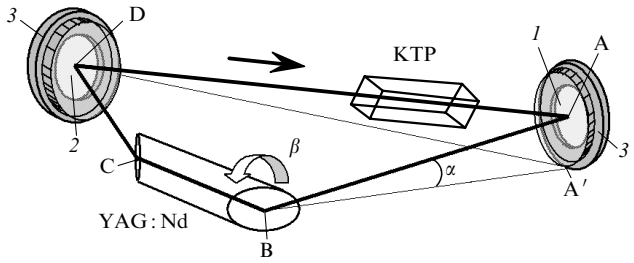

Figure 1. Optical scheme of the Nd : YAG laser resonator: (*1*) output mirror; (*2*) input mirror; (*3*) piezoelectric ceramics.

turned through the angle β with respect to the axis BC to provide the nonplanar geometry. Another surface is cut at a angle providing a decrease in the resonator length and in the distance to mirror (*2*). This mirror is used to couple the pump radiation and has a high reflectivity at 1064 nm. The radii of mirrors (*1*) and (*2*) were 65 and 150 mm, respectively, the distance AD was 49 mm, and the angle of incidence of light on mirrors (*1*) and (*2*) were approximately 10° and 15°, respectively. Such a configuration provided the size of the caustic waist in the Nd : YAG crystal for sagittal and tangential components of the beam equal to 100 and 200 μm, respectively, taking the thermal lens effect into account [8].

We calculated the difference in the intracavity losses for two counterpropagating waves by the Jones matrix method. The coordinates of the point A can be determined by rotating the straight line BA′ through the angle β with respect to the axis CB (the straight line BA′ coincides with the beam incident on the crystal at the Brewster angle in the BCDA′ plane). The rotation angle β corresponds to the nonplanarity angle α (the angle between the straight line AB and the BCDA′ plane). For small angles β, we have $\alpha \approx 0.5\beta$.

In the calculation of the polarisation eigenvectors by the Jones matrix method for a nonplanar geometry, it is necessary to determine the rotations of the coordinate system on passing from one plane to another. The rotation angle of the coordinate system on passing from mirror (*1*) to mirror (*2*) is determined by the angle θ_{12} between the normals to the planes of incidence on mirrors (*1*) and (*2*) [9]:

$$\theta_{12} = \hat{\boldsymbol{a}_1 \boldsymbol{a}_2},$$

where $\boldsymbol{a}_1 = \boldsymbol{n}_1 \times \boldsymbol{k}_1 / \sin\theta_1$; $\boldsymbol{a}_2 = \boldsymbol{n}_2 \times \boldsymbol{k}_2 / \sin\theta_2$; θ_1 and θ_2 are the angles of incidence on the mirrors; $\boldsymbol{k}_i$ are the wave vectors; and $\boldsymbol{n}_1$ and $\boldsymbol{n}_2$ are the normals to the mirror surfaces.

For clockwise and counter-clockwise round trips of radiation in the resonator, we obtain the expressions in the matrix form

$$M_C R(\theta_{BC} + \gamma) M_B R(-\theta_{BA}) M_A R(\theta_{AD}) M_D R(-\theta_{CD}),$$

$$R(-\theta_{CD}) M_D R(\theta_{AD}) M_A R(-\theta_{BA}) M_B R(\theta_{BC} - \gamma) M_C,$$

where θ_{ij} are the moduli of the rotation angles of the coordinate system upon the beam propagation from the point i to j; M_A, and M_D are the Jones matrices for mirrors (*1*) and (*2*), respectively; M_C is the partial polariser matrix describing the characteristics of the antireflection coating of the crystal face (in the ideal case, M_C is the unit matrix); R are the rotation matrices of the coordinate system; $\gamma = V l_{YAG} \boldsymbol{k}\boldsymbol{B}$ is the rotation angle of the polarisation azimuth caused by the Faraday effect; $V = 1.80 \times 10^{-7}$ rad mm^{-1} G^{-1} is the Verdet constant for the Nd : YAG crystal at a wavelength of 1064 nm; l_{YAG} is the crystal length; $\boldsymbol{B}$ is the magnetic induction;

$$M_B = \begin{pmatrix} 1 & 0 \\ 0 & \dfrac{2n}{1+n^2} \end{pmatrix}$$

is the partial polariser matrix (for one surface oriented at the Brewster angle); and n is the refractive index.

The dependences of the intracavity losses introduced by a nonreciprocal element on the rotation angle β for clockwise and counter-clockwise propagating light waves are presented in Fig. 2. The resulting difference of losses between clockwise and counter-clockwise waves was $\sim 0.4\,\%$ for $\beta \approx 8°$ and minimal losses for one of the directions. The magnetic field strength used in calculations was 5.5 kG for the crystal length $l_{YAG} = 8.5$ mm, while the reflectivity of mirrors for the s- and p-polarisation components were unity.

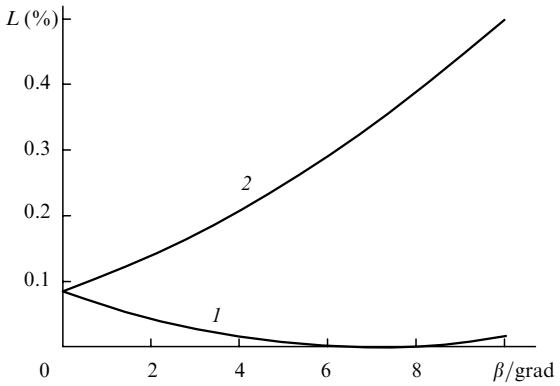

Figure 2. Resonator losses L introduced by an optical diode during the clockwise (*1*) and counter-clockwise (*2*) propagation of light waves in the resonator.

2.2 Selection of competing lines by a birefringent selector

The second harmonic was generated in a KTP crystal placed in the resonator. The eo – e type of noncritical phase matching in the XY plane was used, and KTP Z axis was oriented at 45° to the direction of fundamental radiation polarisation in the resonator. This orientation of the crystal allows us to use it as a birefringent optical element for tuning the laser frequency by varying temperature.

The laser crystal surface oriented at the Brewster angle played the role of a polarisation element. In this case, linear polarisation specified by the polarisation element is divided in the birefringent crystal into the ordinary and extraordinary components, having different refractive indices in the crystal. As a result, an optical path difference appears between the ordinary and extraordinary waves. For the

radiation frequencies at which the optical path difference is equal to an integer of wavelengths, polarisation at the output of the birefringent crystal remains invariable. The wavelengths for which the losses introduced by the birefringent selector will be minimal are determined by the expression

$$q\lambda = l(T)[n_e(\lambda, \varphi, \theta, T) - n_o(\lambda, \varphi, \theta, T)],$$

where q is an integer (the number of the selector mode); l is the birefringent crystal length; n_o and n_e are the refractive indices for the ordinary and extraordinary beams; φ is the angle determining the direction in the crystal in the XY plane with respect to the X axis; θ is the angle determining the direction in the crystal with respect to the Z axis; and T is the crystal temperature.

The dependence of the refractive indices of the KTP crystal on temperature allows one to control the position of transmission maxima of the filter and, hence, the radiation frequency of the laser by varying the crystal temperature. A large width of the temperature phase matching of the KTP crystal ($\sim$25 K cm^{-1}) permits the intracavity second-harmonic generation within the tuning range of the birefringent filter.

In the presence of two competing laser lines of different intensities in the gain medium (for example, a strong line at $\lambda_1 = 1064.25$ nm and a weak line at $\lambda_2 = 1061.54$ nm for the Nd : YAG laser), the length of the birefringent crystal should be properly chosen. To generate only a strong line, it is necessary that, upon tuning of one of the modes of the birefringent selector to the maximum of a strong line, another mode with the number q_2 would be at the maximum of a weak line. It is obvious that in this case lasing cannot occur at a weak line. To obtain lasing at a weak line when one of the modes of the selector (with the number q_2) is tuned to its centre, the other selector modes should be located as far as possible from the strong line centre. The optimal is the case when the centre of a strong line is located exactly between two modes of the selector, i.e., the effective value of q_1 is $\kappa - 1/2$, where κ is an integer. In this case, lasing can occur at a weak line.

In the case of lasing at a strong line, the birefringent crystal length can be found from the condition

$$q_1 - q_2 = \frac{l[n_e(\lambda_1, \varphi, \theta, T) - n_o(\lambda_1, \varphi, \theta, T)]}{\lambda_1}$$

$$- \frac{l[n_e(\lambda_2, \varphi, \theta, T) - n_o(\lambda_2, \varphi, \theta, T)]}{\lambda_2} = \kappa.$$

Lasing at a weak line can occur when the birefringent crystal length satisfies the condition

$$q_1 - q_2 = \frac{l[n_e(\lambda_1, \varphi, \theta, T) - n_o(\lambda_1, \varphi, \theta, T)]}{\lambda_1}$$

$$- \frac{l[n_e(\lambda_2, \varphi, \theta, T) - n_o(\lambda_2, \varphi, \theta, T)]}{\lambda_2} = \kappa - 1/2.$$

The optimal lengths of the KTP crystal in our case (for $\kappa = 1$, 2, 3) for lasing at $\lambda_1 = 1064.25$ nm and $\lambda_2 = 1061.54$ nm and intracavity SHG are, respectively: $l_1 = 4.35$, 8.7, and 13.5 mm (for the orientation angles of the KTP crystal $\theta = 90^\circ$ and $\varphi = 23.5^\circ$) and $l_2 = 2.17$, 6.5, and 10.84 mm (for $\theta = 90^\circ$ and $\varphi = 26.1^\circ$).

To obtain the maximum SHG power by tuning the laser within the gain line, we used the KTP crystal of length 8.7 mm. To realise temperature tuning, the laser resonator was mounted on a thermoelectric element. The good thermal conduction of the construction provided efficient heat transfer to the KTP crystal. Figure 3 shows the experimental temperature dependence of the laser wavelength (wave number) for the KTP crystal of length 8.7 mm. We obtained the tuning of the laser within 700 GHz in the vicinity of 532 nm. The SHG output power at the centre of the tuning curve was above 160 mW upon pumping by a 3-W diode laser.

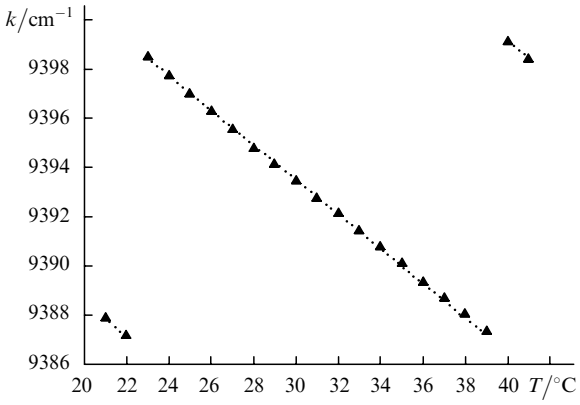

Figure 3. Dependence of the wave number of the Nd : YAG laser radiation on the 8.7-mm KTP crystal temperature.

3. Stabilisation of the Nd : YAG laser frequency by saturation absorption resonances in a luminescence cell with molecular iodine by using second harmonic

At present, many methods of ultrahigh-resolution laser spectroscopy are developed, in which information on the interaction of radiation with a medium is obtained in different ways. The methods based on the detection of parameters of radiation interacting with an absorbing medium are, as a rule, inferior with respect to the signal-to-noise ratio in the case of small absorption coefficients. Only a small fraction of radiation is involved in the interaction, and the signal is observed against a rather intense background, so that it is more convenient to detect the radiation power absorbed by the medium. The best results are achieved in the methods in which the signal is measured by detecting particles in an excited state. One of such methods, proposed by Basov and Letokhov [3], uses the observation of luminescence resonances.

The advantages of this method for recording resonances for frequency stabilisation is the possibility of using ultimately narrow resonances, a low optical density in a cell allowing the elimination of parasitic effects caused by variations in the radiation parameters in the cell, and a comparatively small size of the cell (in a short cell, it is easier to form a plane radiation front and eliminate frequency shifts depending on the wave-front curvature). These advantages make it possible to improve the long-term

stability and reproducibility of the laser frequency. The disadvantage of the luminescence method is the complexity of collection of the luminescence signal.

3.1 Scheme of the optical Nd : YAG/I_2 frequency standard with an external absorbing luminescence cell

The block scheme of a Nd : YAG laser stabilised by means of an external absorbing luminescence cell is shown in Fig. 4. To produce saturated absorption resonances, a standing wave at 532 nm was generated in the cell. The luminescence signal was detected with a FU-125 photomultiplier with the multialkali photocathode diameter of 170 mm. To increase the collection of the luminescence signal, a cylindrical reflector was used. An OS-13 optical filter was used to suppress the 532-nm radiation from the laser. The absorbing cell length and diameter were 400 and 30 mm, respectively. The cell windows were oriented at the Brewster angle. To control the operating pressure, the cell had a cold finger with iodine crystals placed into a temperature controller. The temperature controller provided the temperature stability of the cold finger of $\sim 10^{-2}$ °C.

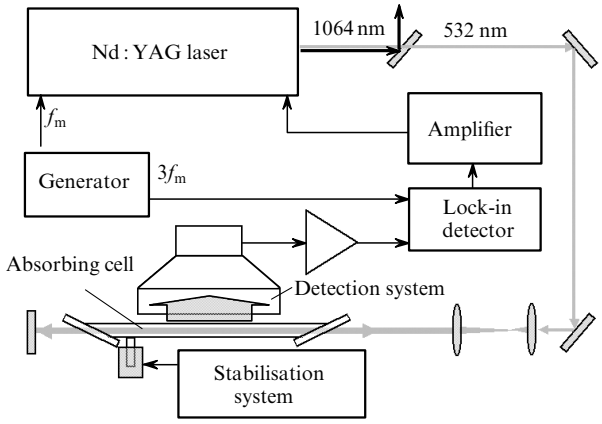

Figure 4. Block scheme of the Nd : YAG laser frequency-stabilised by means of an external absorbing luminescence cell (f_m is the modulation frequency).

The laser resonator mirrors were mounted on piezoelectric drives, allowing the control of the resonator length by means of electric signals. The error signal was obtained by modulating the radiation frequency of the laser at ~ 500 Hz. The automatic control system operated using the central zero of the third derivative of the nonlinear resonance line, which provided the minimisation of the frequency shift due to a sloping pedestal caused by the adjacent hyperfine-structure components. The obtained error signal was fed to another piezoelectric ceramics (see Fig. 1) to tune automatically the laser frequency to the nonlinear resonance frequency.

We used a low probe-modulation frequency because the main contribution to the nonlinear resonance at low pressures of molecular iodine comes from the lower energy level, whose relaxation time is close to the flight time of a molecule through the light beam. It is known that when the scan rate is comparable with the relaxation time of one of the levels involved in the transition, the even harmonics of the modulation frequency appear in the signal due to different saturation during the scan period. In the presence of a sloping pedestal, the odd harmonics appear, including the third one, resulting in the shift of the third-harmonic zero of the nonlinear resonance. Figure 5 shows nonlinear resonances observed for different laser scan frequencies f. One can see that for modulation frequencies $f_m = 1$ kHz and above, the signal shape is distorted.

3.2 Long-term frequency stability of Nd : YAG lasers

The setup for measuring the frequency stability and reproducibility of frequency-stabilised Nd : YAG lasers consisted of two independent systems.

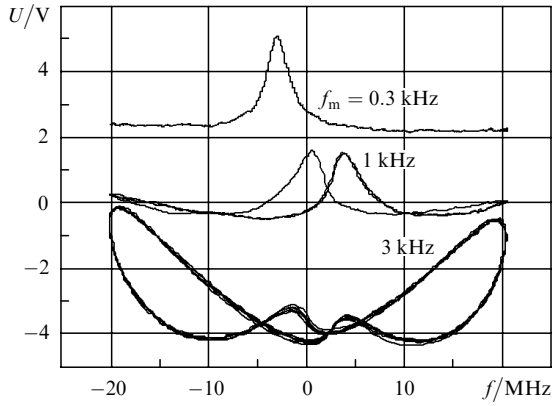

Figure 5. Nonlinear resonances observed at different laser scan rates f.

Both Nd : YAG lasers were stabilised by the saturated absorption resonance in molecular iodine at the hyperfine-structure component a_1 of the $X(v'' = 0, J'' = 56) \rightarrow B(v' = 32, J' = 57)$ transition with the minimum natural width. We measured the beat frequency of the Nd : YAG lasers at nonzero frequencies by using two acousto-optic frequency modulators operating at 80 and 81 MHz. Therefore, the beat signal was detected at the frequency 1 MHz. The operating frequencies of the acousto-optic modulators were synthesised from the hydrogen frequency standard.

By processing the experimental data, we constructed the Allan function $\sigma(2, \tau)$ (Fig. 6). One can see that the relative long-term frequency stability of the Nd : YAG lasers during the time $\tau \geqslant 200$s is better than 10^{-14}.

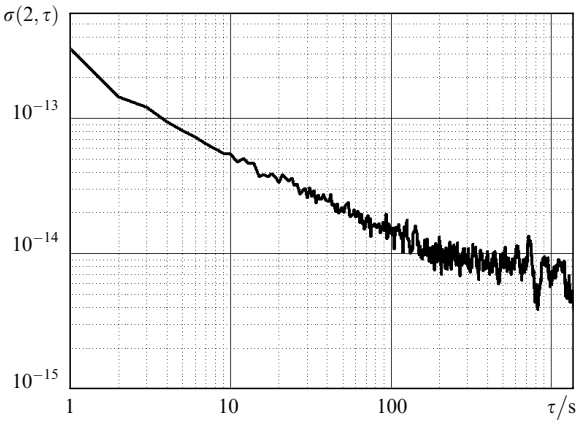

Figure 6. Allan function for the frequency-stabilised Nd : YAG lasers.

4. Effect of the operating parameters of an absorbing cell on the frequency shift of a laser stabilised by saturated absorption resonances in molecular iodine

We investigated the effect of operating parameters of an absorbing cell on the frequency shift of the Nd : YAG laser stabilised by saturated absorption resonances in molecular iodine by varying a parameter in one of the systems and measuring a change in the difference beat frequency of the two lasers with different parameters. We investigated the frequency shift of saturated absorption resonances for the component a_2 of the $R(56)$ 32–0 line as a function of the operating pressure of molecular iodine (Fig. 7). The shift $\Delta\nu/\Delta p$ was $-555(26)$ Hz mTorr^{-1}. We also determined the broadening of saturated absorption resonances for the same component as a function of the molecular iodine pressure (Fig. 8). The pressure dependence of the broadening was 6.5(0.2) kHz mTorr^{-1}.

We studied the dependences of the frequency shift on the power density in an absorbing cell, the probe modulation frequency signal, and the angle between counterpropagating waves producing a standing wave in the absorbing cell. The results are presented below.

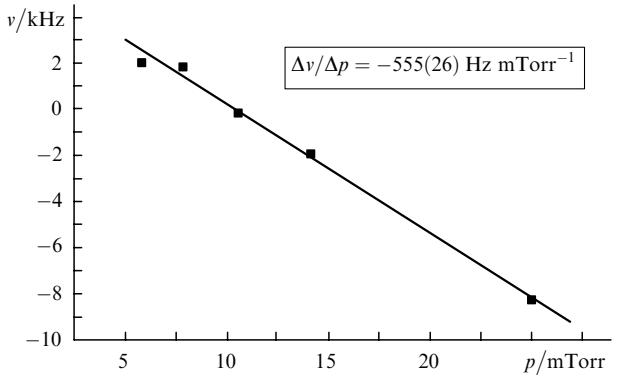

Figure 7. Frequency shift of saturated absorption resonances for the a_2 component of the $R(56)$ 32–0 line as a function of the operating pressure of molecular iodine.

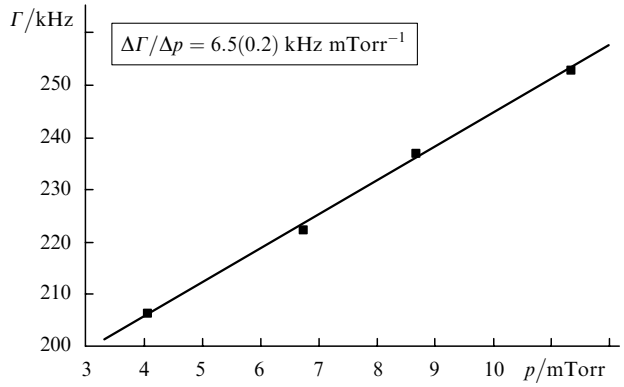

Figure 8. Broadening Γ of saturated absorption resonances for the a_2 component of the $R(56)$ 32-0 line as a function of the operating pressure of molecular iodine.

The frequency shift observed upon changing:

the molecular iodine pressure ..... $\Delta\nu/\Delta p = -555(26)$ Hz mTorr^{-1}
the temperature controlling molecular iodine pressure (near $T = -5$ °C)..... $\Delta\nu/\Delta T = -830$ Hz °C^{-1}
the power in the absorbing cell by a factor of two ..... $\Delta\nu \approx 200$ Hz
the probe modulating signal amplitude by a factor of two ..... $\Delta\nu \approx 1700$ Hz
the angle between counterpropagating waves (near $\psi = 1$ mrad)..... $\Delta\nu/\Delta\psi \approx 9.3$ Hz mrad^{-1}

Based on these studies, we estimated the reproducibility of the frequency of the Nd : YAG laser stabilised by saturated absorption resonances in molecular iodine by using an external absorbing luminescence cell. The expected frequency reproducibility $\nu/\Delta\nu$ is $\sim 3 \times 10^{13}$ for the operating parameters of the system controlled with an accuracy of 10 %.

Figure 9. Transportable frequency standard based on the Nd : YAG/I_2 system.

5. Conclusions

The development and optimisation of the methods for stabilising the Nd:YAG laser frequency by saturated absorption resonances in molecular iodine make it possible to create optical frequency and wavelength standards with the sufficiently high long-term frequency stability and reproducibility and good operating parameters. Small dimensions and a simple design of frequency standards based on the Nd : YAG/I_2 systems allow the development of transportable frequency standards. Figure 9 demonstrates the transportable frequency standard developed at the Institute of Laser Physics, Siberian Branch, RAS.

References

1. Nevsky A.Yu., Holzwarth R., Reichert J., Udem Th., Hänsch T.W., von Zanthier J., Walther H., Schnatz H., Riehl F., Pokasov P.V., Skvortsov M.N., Bagayev S.N. *Opt. Commun.*, **192**, 263 (2001).
2. Hall J.L., Ma Long-Sheng, Taubman M., Tiemann B., Hong Feng-Lei, Pfister O., Ye J. *IEEE Trans. Instr. Meas.*, **48** (2), 583 (1999).
3. Basov N.G., Letokhov V.S. *Electron. Technology*, **2** (2), 15 (1969).

4. Chebotayev V.P., Goncharov A.N., Ohm A.E., Skvortsov M.N. *Metrologia*, **27**, 61 (1990).
5. Kravtsov N.V., Nanii O.E. *Kvantovaya Elektron.*, **20**, 322 (1993) [*Quantum Electron.*, **23**, 272 (1993)].
6. Okhapkin M.V., Skvortsov M.N., Belkin A.M., Kvashnin N.L., Bagayev S.N. *Opt. Commun.*, **203**, 359 (2002).
7. Maker G.T., Malcolm G.P.A., Ferguson A.I. *Opt. Lett.*, **18**, 1813 (1993).
8. Franchiser J., Albers P., Weber H.P. *IEEE J. Quantum Electron.*, **28** (4), 1046 (1992).
9. Chow W.W., Hamberne J.B., Hutchings T.J., Sunders V.E., Sargent III M., Scully M.O. *Rev. Mod. Phys.*, **57** (1), 84 (1985).